

FSDP: Fast and Safe Data-Driven Overtaking Trajectory Planning for Head-to-Head Autonomous Racing Competitions

Cheng Hu^{1*}, Jihao Huang^{1*}, Wule Mao^{1*}, Yonghao Fu^{1*}, Xuemin Chi¹, Haotong Qin^{2†},
Nicolas Baumann², Zhitao Liu¹, Michele Magno², and Lei Xie^{2†}

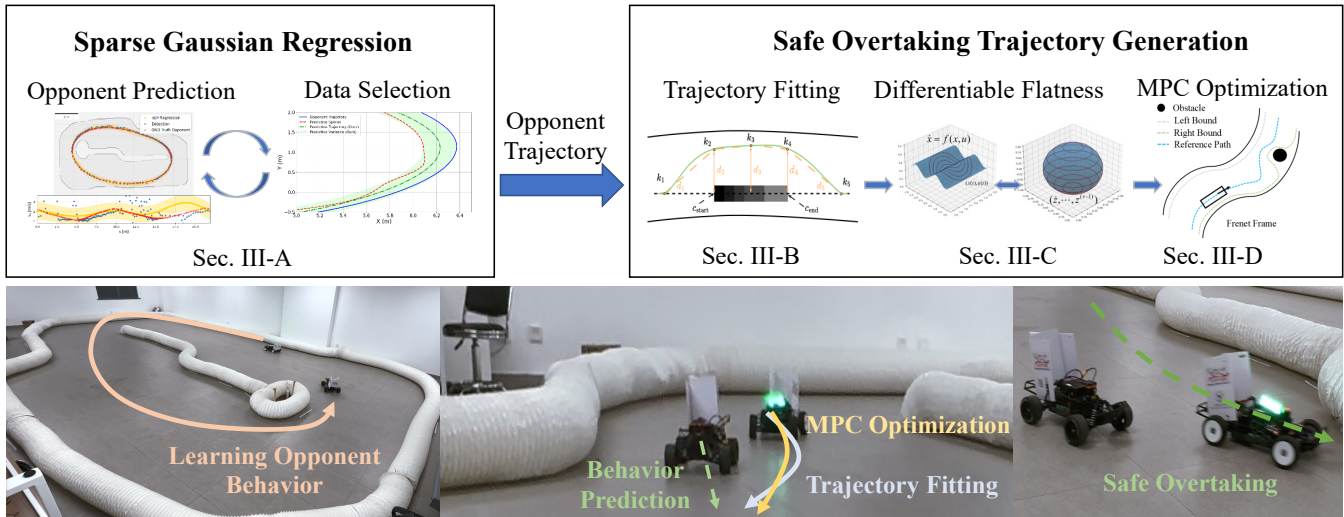


Fig. 1: Framework of the proposed *Fast and Safe Data-Driven Planner*: The proposed method first employs the Sparse Gaussian Process (SGP) to learn the opponent’s behavior and predict its trajectory. Based on this prediction, a bi-level Quadratic Programming (QP) planner generates an overtaking trajectory that ensures both kinematic feasibility and safety.

Abstract—Generating overtaking trajectories in autonomous racing is a challenging task, as the trajectory must satisfy the vehicle’s dynamics and ensure safety and real-time performance running on resource-constrained hardware. This work proposes the *Fast and Safe Data-Driven Planner* to address this challenge. Sparse Gaussian predictions are introduced to improve both the computational efficiency and accuracy of opponent predictions. Furthermore, the proposed approach employs a bi-level quadratic programming framework to generate an overtaking trajectory leveraging the opponent predictions. The first level uses polynomial fitting to generate a rough trajectory, from which reference states and control inputs are derived for the second level. The second level formulates a model predictive control optimization problem in the Frenet frame, generating a trajectory that satisfies both kinematic feasibility and safety. Experimental results on the F1TENTH platform show that our method outperforms the State-of-the-Art, achieving an 8.93% higher overtaking success rate, allowing the maximum opponent speed, ensuring a smoother ego trajectory, and reducing 74.04% computational time compared to the *Predictive Spliner* method. The code is available at: <https://github.com/ZJU-DDRX/FSDP>.

* Equal contribution.

¹ Authors are associated with the Department of Control Science and Engineering, Zhejiang University.

² Authors are associated with the Center for Project-Based Learning, D-ITET, ETH Zurich.

[†] Corresponding Authors haotong.qin@pbl.ee.ethz.ch, lxie@iipc.zju.edu.cn.

I. INTRODUCTION

Autonomous racing serves as a high-intensity testbed for advancing general autonomous by pushing autonomy algorithms to their limits under extreme conditions [1], [2]. In recent years, competitions such as Formula Student Driverless (FSD), the Indy Autonomous Challenge (IAC), and the scaled-down F1TENTH races have gained popularity [3], [4]. While full-scale events like FSD and IAC impose constraints on overtaking due to cost considerations, scaled autonomous racing, such as F1TENTH, enables unrestricted overtaking. Success in scaled autonomous racing depends on effective overtaking strategies, requiring autonomous vehicles to drive at peak speed and navigate around competitors. Unlike highway overtaking, where vehicle dynamics are stable and predictable, autonomous racing involves vehicles operating at the limits of grip, making overtaking a unique and complex challenge [5].

The methods for planning overtaking trajectories can be primarily divided into two approaches: end-to-end direct trajectory generation and traditional hierarchical planning [2]. Although some end-to-end overtaking methods based on reinforcement learning have been validated in commercial vehicles [6], simulations [7], and scaled-down racing cars [8], [9], in real-world racing environments, such as the Abu Dhabi Racing League (A2RL) [10], the high-speed collisions

and costly repair expenses pose significant risks. As a result, current approaches in real-world applications still rely on more traditional methods involving perception, planning, and control. From a hierarchical perspective, the main challenge lies in planing a collision-free overtaking trajectory while considering predicting the opponent’s trajectory at the friction limit.

Planning such a trajectory at high speeds involves three significant challenges: 1) **Opponent Prediction:** The trajectory must account for the future behavior of the overtaken vehicle, as sudden lateral movements for opponent avoidance could result in loss of control and potential sliding; 2) **Overtaking Feasibility:** The planned trajectory must adhere to fundamental vehicle dynamics without collision, ensuring that the low-level controller can track it accurately; 3) **Real Time Requirements:** Overtaking opportunities are brief at high speeds, making the efficiency of the planning solution critical for success.

To address these challenges, this paper proposes the *Fast and Safe Data-Driven Planner* (FSDP) for overtaking, which uses the Sparse Gaussian Process (SGP) to fit the opponent’s behavior online. By combining Gaussian predictions with the vehicle’s dynamics, FSDP generates a collision-free and feasible overtaking trajectory with a bi-level Quadratic Programming (QP) planner. The main contributions of this paper are summarized as follows:

- I **Sparse Gaussian Process (GP) based Prediction:** SGP is utilized for real-time fitting of the opponent’s trajectory and velocity, while its integration with K-means clustering enables efficient and accurate dataset updates. This approach reduces prediction time by 60.53% and enhances prediction accuracy by 33.87% compared to previous methods [11].
- II **Fast and Safe Overtaking Planning:** A bi-level QP framework is used to efficiently generate a smooth and collision-free overtaking trajectory. Both QP optimizations incorporate opponent prediction information from SGP. The first QP provides a smooth initial trajectory via polynomial fitting. Based on Model Predictive Control (MPC), the second QP ensures kinematic feasibility and enforces safety using collision avoidance constraints in the Frenet frame. This enables FSDP to achieve an 8.93% higher overtaking success rate over [11] with the maximum opponent speed.
- III **Open Source:** The proposed FSDP was tested and compared with State-of-the-Art (SOTA) methods in simulations and on the F1TENTH car platform. The complete code has been made open-source to enhance reproducibility [4].

II. RELATED WORK

The existing overtaking planning methods in the context of autonomous racing can be mainly divided into two categories: sampling-based overtaking and optimization-based overtaking.

A. Sampling Based Path-Planning

Sampling-based planning methods primarily generate numerous candidate trajectories, followed by the design of a cost function to select the overtaking trajectory that meets the desired requirements. The candidate trajectory generation methods can be both real-time and offline. The *Frenet Planner* [12] generates multiple trajectories online in the Frenet coordinate system. Then the cost function is designed to penalize deviations from the racing line and to avoid current opponents. A classic offline candidate trajectory generation method used in autonomous racing is called Graph-Based Overtake (GBO) [13]. This method generates candidate trajectories offline by defining nodes in a known map using a lattice and connecting the nodes with splines. Although sampling-based methods can efficiently generate overtaking trajectories, the choice of cost function and the number of sampling points can significantly impact the quality of trajectory generation. Additionally, the generated trajectories do not account for the future movement of opponents, which may lead to frequent changes in overtaking behavior and result in substantial computational requirements.

FSDP addresses these challenges by predicting the movement of the opponent car using Gaussian processes and incorporating this information into the QP optimization problem of the MPC, significantly enhancing safety.

B. Optimization-Based Overtaking

Optimization-based overtaking methods involve solving a real-time optimization problem with collision avoidance constraints.

Model Predictive Contouring Control (MPCC) is an overtaking method that integrates both planning and control. Unlike methods that rely on a reference racing line, MPCC aims to maximize the vehicle’s progress along the centerline, incorporating the opponent car as an obstacle within the optimization problem [14]. It focuses solely on minimizing lap time while ensuring collision-free operation within the map. However, the performance of this method is highly sensitive to the parameters, and the controller also experiences a significant computational burden.

Another approach is to use polynomials as model constraints while treating the opponent as an obstacle in the optimization. A prominent example in racing is *Spliner* [4]. This method fits a simple first-order polynomial in the Frenet coordinate system. Its advantages include high real-time performance and a high success rate of solving. *Predictive Spliner* [11] utilizes standard Gaussian processes to predict the trajectory and velocity of the opponent car. In the *Spliner* optimization problem, the predicted collision intervals are considered to avoid collision, thereby achieving a higher overtaking success rate. This method has been successfully validated in the F1TENTH competition and is currently one of the SOTA approaches. However, as the Gaussian dataset grows, both training and prediction times increase accordingly. Using only the most recent data to construct the dataset results in losing historical information about the

Algorithm	Fast Opp. Pre	Kine. Feasibility	Param. Sensitivity	Compute
Frenet [12]	No	No	Low	Low
GBO [13]	No	No	High	Low
Spliner [4]	No	No	Low	Low
Pred. Spliner [11]	No	No	Low	Medium
FSDP (ours)	Yes	Yes	Low	Low

TABLE I: Summary of existing overtaking strategies, denoting key characteristics of each method; *Fast Opponent Prediction* considerations (desired yes); *Kinematic model feasibility* is satisfied by the overtaking trajectory (desired yes); Susceptibility to *Parameter Sensitivity* (desired low); Nominal Computational load (desired low).

opponent car. Although the sensitivity of the polynomial-based *Spliner* parameters is significantly lower compared to the dynamics-based MPCC, the generated trajectories may not be suitable for tracking by the low-level controller [15].

FSDP addresses these issues by employing sparse Gaussian processes to fit the trajectory and velocity of the opponent car and designing a distance function based on induced points to filter and update the data. Additionally, the MPC utilizes a linearized kinematic model through differential flatness, enhancing both the feasibility of the trajectory and the computational efficiency of the solution.

C. Summary of Existing Overtaking Algorithms

Table I summarizes the comparison between the method proposed in this paper and SOTA methods.

III. METHODOLOGY

In this section, we provide a detailed illustration of how FSDP operates. First, we use SGP to predict the behavior of the opponent. Next, we demonstrate how to obtain an initial rough trajectory through polynomial fitting and differential flatness techniques. Finally, MPC is employed to ensure the vehicle’s kinematic feasibility and enforce strict safety constraints. The structure of FSDP can be seen in Fig. 1.

A. Sparse GP-Based Opponent Prediction

1) *Opponent Prediction with Sparse GP*: In the context of autonomous racing competitions, when a vehicle is in a trailing state, the perception system collects data on the position and speed of the opponent vehicle [4]. *Predictive Spliner* [11] uses a standard GP for fitting and prediction. Assume the dataset size is N , with input and output dimensions being n_z and n_d , respectively. The computational complexities for calculating the mean and variance are $\mathcal{O}(n_d n_z N)$ and $\mathcal{O}(n_d n_z N^2)$. The proposed method uses SGP with M inducing points ($M \ll N$) to approximate the low-dimensional kernel matrix, mapping $\mathbb{R}^{N \times N}$ to $\mathbb{R}^{M \times M}$. The computational complexities for mean and variance become $\mathcal{O}(n_d n_z M)$ and $\mathcal{O}(n_d n_z M^2)$ [16]. Therefore, SGP achieves fast fitting and prediction.

The choice of the sparse Gaussian method is based on Variational Free Energy (VFE) [16]. This method involves jointly inferring the inducing points and the hyperparameters by maximizing a lower bound of the marginal likelihood. Specifically, the approximate posterior is assumed to be $q(\mathbf{f}, \mathbf{f}_z | \mathbf{Y}) = p(\mathbf{f} | \mathbf{f}_z) \phi(\mathbf{f}_z)$, where \mathbf{f} represents the latent

function, \mathbf{f}_z denotes the latent function at the inducing points \mathbf{Z}_m , \mathbf{Z} is the input of the training data, and \mathbf{Y} represents the noisy outputs. $\phi(\mathbf{f}_z)$ is a variational distribution over \mathbf{f}_z . This assumption enables a critical cancellation that results in a computationally tractable lower bound \mathcal{F}_V . After obtaining the optimal lower bound, the mean and covariance function of the approximate posterior at test point z^* are obtained as follows:

$$\mu^v(z^*) = (\Sigma^\omega)^{-1} K_{z^* \mathbf{Z}_m}(\mathcal{W}) K_{\mathbf{Z}_m \mathbf{Z}} \mathbf{Y} \quad (1)$$

$$\Sigma^v(z^*) = K_{z^* z^*} - Q_{z^* z^*} + K_{z^* \mathbf{Z}_m}(\mathcal{W}) K_{\mathbf{Z}_m z^*} \quad (2)$$

where $\mathcal{W} = (K_{\mathbf{Z}_m \mathbf{Z}_m} + (\Sigma^\omega)^{-1} K_{\mathbf{Z}_m \mathbf{Z}} K_{\mathbf{Z} \mathbf{Z}_m})^{-1}$.

The travel distance s_{opp} , lateral error d_{opp} , and velocity v_{opp} of the opponent car on the reference trajectory in the Frenet coordinate system are obtained through the perception system [4]. Using s as the input, two sparse Gaussian models, denoted as $\text{SGP}_d(s)$ and $\text{SGP}_v(s)$, are constructed with d and v as the outputs, respectively.

2) *Data Selection*: In *Predictive Spliner*, the GP always uses the latest dataset for fitting and prediction, ignoring the information from old data. In contrast, our data selection method strategically constrains the dataset size N_{target} while integrating both new observations and old data to achieve robust fitting of the preceding vehicle’s trajectory.

We construct two SGP models with the input being the travel distance s , and the outputs corresponding to the lateral error d and the speed v , respectively. To facilitate the description of the data selection method, we will use the following notation: Given the training set $\mathcal{D}_{\text{train}} = \{(\mathbf{x}_i, \mathbf{y}_i)\}_{i=1}^{N_{\text{train}}}$ and the incoming data $\mathcal{D}_{\text{incoming}} = \{(\mathbf{x}_j, \mathbf{y}_j)\}_{j=1}^{N_{\text{incoming}}}$, where \mathbf{x} is the input feature vector and \mathbf{y} is the corresponding target value vector. Then, three methods are employed to conduct preliminary filtering of the data.

First, the *Time-based Spatial Filter* calculates the spatial bins independently for each lap and selects the maximum timestamp within each spatial bin:

$$\mathcal{D}_{\text{filtered}} = \bigcup_{k=1}^{\lceil L/\Delta s \rceil} \left\{ \arg \max_{(\mathbf{x}, \mathbf{y}, t) \in \mathcal{S}_k} t \right\} \quad (3)$$

where L is total trajectory length, Δs is spatial bin width proportional to waypoint density, \mathcal{S}_k is k -th spatial bin, and t is the timestamp of data point.

Second, the *Range Filter* ensures that data points are within a predefined range of values $[y_{\min}, y_{\max}]$.

Third, the *Confidence Interval Filter* applies when $N_{\text{train}} > \frac{2}{3} N_{\text{target}}$, checking if the data points fall within the 95% confidence interval of the original SGP.

When using Leave-One-Out Variances with GP or SGP to describe the information richness of the data, it is necessary to solve the inverse matrix of the new kernel at each step. The proposed method, which utilizes inducing points \mathbf{Z}_m to describe the predictive distance of different points, significantly improves the real-time performance. A smaller distance indicates that the information contained in the two points is more similar, as shown in the following equation:

$$\sigma_s^2(\mathbf{x}_j) = k(\mathbf{x}_j, \mathbf{x}_j) - \mathbf{k}_{\mathbf{x}_j \mathbf{Z}_m} \mathbf{K}_{\mathbf{Z}_m \mathbf{Z}_m}^{-1} \mathbf{k}_{\mathbf{Z}_m \mathbf{x}_j} + \Sigma^\omega \quad (4)$$

where $k(\cdot, \cdot)$ is kernel function and Σ^ω is observation noise variance.

After data filtering, new data can only be added to the dataset if its predictive distance exceeds the average distance of the training data. This step aims to ensure that the dataset contains information-rich points, as described by the following equation:

$$\sigma_s^2(\mathbf{x}_j) > \frac{1}{N_{\text{train}}} \sum_{i=1}^{N_{\text{train}}} \sigma_s^2(\mathbf{x}_i) \quad (5)$$

where $\sigma_s^2(\mathbf{x}_j)$ is predictive variance at \mathbf{x}_j from Eq. (4).

The pruning process is activated only if the merged dataset $D_{\text{merged}} = D_{\text{train}} \cup D_{\text{filtered}}$ exceeds the preset size N_{target} . First, K-means clustering is performed using the SGP's inducing points \mathbf{Z}_m as initial centroids, partitioning D_{merged} into K clusters (where K equals the number of inducing points M). The clustering objective is:

$$\min_{\{c_k\}} \sum_{k=1}^K \sum_{x \in c_k} \|x - z_{m,k}\|^2 \quad (6)$$

where $z_{m,k}$ represents the k -th inducing point.

Next, the mean predictive distance $\bar{\sigma}_{s,k}^2$ within each cluster C_k is calculated. Data points with variances below $\bar{\sigma}_{s,k}^2$ are removed. If the global dataset size remains larger than N_{target} after this step, additional points are pruned proportionally from each cluster until the target size is reached.

Algorithm 1 Inducing-Guided Data Selection

1: **Input:** $D_{\text{train}}, D_{\text{incoming}}$ **Output:** D_{pruned}
2: **Filtering:**
3: **for** each lap **do**
4: Sort \mathcal{D} by Δs , keep latest point in each bin
5: **end for**
6: $D_{\text{filtered}} = \{\mathbf{x}_j, y_j \in D_{\text{incoming}} \mid y_j \in [y_{\min}, y_{\max}]\}$
7: **if** $|D_{\text{train}}| > \frac{2}{3}N_{\text{target}}$ **then**
8: Retain $y \in [\mu(x) \pm 1.96\sigma^2(x)]$ for $(x, y) \in D_{\text{filtered}}$
9: **end if**
10: **Adding New Data:**
11: Keep $\sigma_s^2(x) > \frac{1}{|D_{\text{train}}|} \sum \sigma_s^2(D_{\text{train}})$ for $x \in D_{\text{filtered}}$
12: $D_{\text{merged}} \leftarrow D_{\text{train}} \cup D_{\text{filtered}}$
13: **Pruning:**
14: **if** $|D_{\text{merged}}| \geq N_{\text{target}}$ **then**
15: Cluster D_{merged} via K-means(\mathbf{Z}_m)
16: **for** each cluster C_k **do**
17: Prune \mathbf{x} where $\sigma_s^2(\mathbf{x}) < \frac{1}{|C_k|} \sum \sigma_s^2(C_k)$
18: Keep top $\lfloor N_{\text{target}} \cdot \frac{|C_k|}{|D_{\text{merged}}|} \rfloor$ points
19: **end for**
20: **end if**

3) *Collision Prediction:* Let $s_{\text{ego}}(k)$ and $s_{\text{opp}}(k)$ represent the positions of the ego and opponent vehicles at time k . The time interval and prediction horizon are defined as Δt and

T_N . The forward simulation of the vehicles is shown below:

$$\begin{aligned} s_{\text{ego}}(k+1) &= s_{\text{ego}}(k) + v_{\text{ego}}(k)\Delta t + \frac{1}{2}a_{\text{ego}}(k)\Delta t^2 \\ v_{\text{ego}}(k+1) &= v_{\text{ego}}(k) + a_{\text{ego}}(k)\Delta t \\ s_{\text{opp}}(k+1) &= s_{\text{opp}}(k) + v_{\text{opp}}(k)\Delta t \\ v_{\text{opp}}(k+1) &= \mathcal{SGP}_v(s_{\text{opp}}(k+1)) \end{aligned} \quad (7)$$

Within the prediction horizon T_N , if the difference in travel distance between the two vehicles is less than the collision threshold s_c , the position of the ego vehicle at the corresponding point $s_{\text{ego}}(k)$ is identified as the start of the collision interval c_{start} . Subsequently, if the difference in travel distance exceeds the collision threshold s_c , the point c_{end} is marked as the end of the collision interval. After obtaining the collision interval, the lateral position of the opponent car can be represented using the SGP model based on the vehicle's position.

$$d_{\text{opp}} = \mathcal{SGP}_d(s), \quad s \in [c_{\text{start}}, c_{\text{end}}] \quad (8)$$

The predicted collision interval provides a safe constraint for generating the overtaking trajectory in the subsequent steps.

B. Efficient QP-Based Initial Trajectory Generation

In this section, a collision-free initial trajectory is rapidly generated by constructing a QP fitting problem. Based on the predicted positions of opponents from SGP, several key points are identified in the Frenet frame, such as k_1, k_2, k_3, k_4 , and k_5 , as shown in Fig. 2. k_1 and k_5 represent the start and end points of the planned trajectory, with the corresponding $d = 0$. k_2, k_3 , and k_4 represent the start, middle, and end points of the predicted opponent trajectory. The d values for k_2, k_3 , and k_4 are then determined, ensuring that the points maintain a distance greater than the safety threshold from the corresponding predicted opponent and do not exceed the track boundaries.

After determining the d coordinates of these key points, linear interpolation is performed to estimate the intermediate d coordinates. These discrete points are used to generate an initial, collision-free trajectory $P^*(t)$. A QP problem is then formulated to refine this trajectory by fitting it with a polynomial, ensuring a smoother trajectory.

The vehicle's position is described by the polynomial $P(t) = \mathbf{k}^\top \boldsymbol{\beta}(t)$, where $t \in [0, T]$, $\mathbf{k} \in \mathbb{R}^{2n}$ is the coefficient vector, and $\boldsymbol{\beta}(t) = [1 \ t \ t^2 \ \dots \ t^{2n-1}]^\top$ is the natural basis. The trajectory is a fifth-degree polynomial since $n = 3$. The trajectory fitting problem can be formulated as a QP problem as follows:

$$\begin{aligned} \min \quad & \int_0^T \|P(t) - P^*(t)\|^2 dt \\ \text{s.t.} \quad & P^{(j)}(T) = P^{*(j)}(T) \\ & P^{(j)}(0) = P^{*(j)}(0), j \in \{0, 1\} \end{aligned} \quad (9)$$

where the constraints include position and velocity constraints at the start and end points.

C. Linearized Reference States Extraction Based on Differential Flatness

After the trajectory represented by the fifth-degree polynomial is obtained, the differential flatness property is used

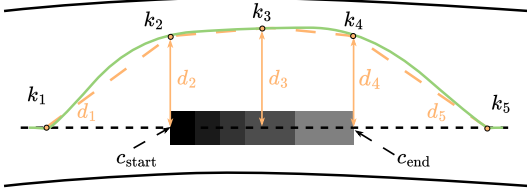


Fig. 2: Schematic diagram of the initial collision-free trajectory. The black region represents the predicted positions of the opponent using SGP. The black dashed line denotes the racing line, while the yellow dashed line illustrates the rough evasion trajectory obtained through key point interpolation. The green trajectory is the smoothed avoidance trajectory obtained from QP.

to find the linearized reference states, facilitating the lower-layer MPC optimization. For the kinematic bicycle model in Cartesian coordinates frame, the state vector $\mathbf{x}_c = [x, y, v, \theta]^\top$, the input vector $\mathbf{u}_c = [a_t, \delta]^\top$ are defined. Where $[x, y]^\top$ is the position at the center of the rear wheel, v is the longitudinal velocity, a_t is the longitude acceleration, and δ is the steering angle. Based on the characteristics of differential flatness, all information is expressed through x and y as follows:

$$\begin{cases} v = \sqrt{\dot{x}^2 + \dot{y}^2} & (10a) \\ \theta = \tan^{-1}(\dot{y}/\dot{x}) & (10b) \\ a_t = (\dot{x}\ddot{x} + \dot{y}\ddot{y})/\sqrt{\dot{x}^2 + \dot{y}^2} & (10c) \\ \delta = \tan^{-1}((\dot{x}\ddot{y} - \dot{y}\ddot{x})L/(\dot{x}^2 + \dot{y}^2)^{\frac{3}{2}}) & (10d) \end{cases}$$

where L is the length of the wheelbase. Thus, the flat outputs $[x, y]^\top$ and their finite derivatives describe the arbitrary state and input information of the vehicle [17]. After selecting the reference points along the trajectory and coordinate transformation, the corresponding states \mathbf{X}_{ref} and control inputs \mathbf{U}_{ref} in the Frenet frame can be obtained using differential flatness. These reference points can then serve as the linearized reference points for MPC in the lower-layer planner.

D. MPC-Based Optimization for Kinematic Feasibility and Safety Guarantee

This section demonstrates the optimization of initial reference trajectory. To satisfy the vehicle's kinematic dynamics and ensure safety, MPC is employed for optimization, and the entire optimization problem is formulated in the Frenet frame to ensure real-time performance. The vehicle's kinematic dynamics are expressed as follows:

$$\begin{cases} \dot{s} = \frac{v \cos \theta}{1 - \kappa_r(s)n}, \quad \dot{n} = v \sin \theta, \\ \dot{\theta} = \frac{v \tan \delta}{L} - \kappa_r(s) \frac{v \cos \theta}{1 - \kappa_r(s)n}, \end{cases} \quad (11)$$

where s denotes the distance traveled along the racing line, θ represents the heading angle error, κ_r represents the reference curvature, and n is the lateral deviation. Suppose $\mathbf{x} = [s, n, \theta]^\top$ and $\mathbf{u} = [v, \delta]^\top$, where $n_x = 3$ and $n_u = 2$ are defined.

Assume the state sequence over the MPC prediction horizon N is denoted by $\mathbf{X} = [\mathbf{x}_1^\top, \dots, \mathbf{x}_N^\top]^\top \in \mathbb{R}^{N \cdot n_x}$,

and $\mathbf{U} = [\mathbf{u}_0^\top, \dots, \mathbf{u}_{N-1}^\top]^\top \in \mathbb{R}^{N \cdot n_u}$ denotes the control inputs sequence. In addition, we define an integrated state $\mathbf{X} = [\mathbf{X}^\top - \mathbf{X}_{\text{ref}}^\top, \mathbf{X}^\top, \mathbf{X}^\top - \mathbf{X}_{\text{pre}}^\top]^\top$, where \mathbf{X}_{ref} denotes the reference states sequence derived from differential flatness, and $\mathbf{X}_{\text{pre}} = [\mathbf{x}_0^\top, \dots, \mathbf{x}_{N-1}^\top]^\top$. The optimization problem is formulated as:

$$\min_{\mathbf{X}, \mathbf{U}} \|\mathbf{X}^* - \mathbf{Q}\|^2 + \|\mathbf{U} - \mathbf{U}_{\text{ref}}\|_{\mathbf{R}}^2 \quad (12a)$$

$$\text{s.t. } \mathbf{x}_k = \mathbf{A}_k \mathbf{x}_{k-1} + \mathbf{B}_k \mathbf{u}_{k-1}, k = 1, 2, \dots, N, \quad (12b)$$

$$l_b(s_k^{\text{ref}}) \leq \mathbf{x}_k(1) \leq u_b(s_k^{\text{ref}}), k = 1, 2, \dots, N, \quad (12c)$$

$$\mathbf{u}_{\min} \leq \mathbf{u}_k \leq \mathbf{u}_{\max}, \Delta \mathbf{u}_{\min} \leq \Delta \mathbf{u}_k \leq \Delta \mathbf{u}_{\max}, \quad (12d)$$

where $\Delta \mathbf{u}_k = \mathbf{u}_k - \mathbf{u}_{k-1}$, and \mathbf{A}_k and \mathbf{B}_k are the linearized system matrices evaluated at the reference points $\mathbf{x}_{k,\text{ref}}$ and $\mathbf{u}_{k-1,\text{ref}}$. \mathbf{U}_{ref} represents the reference control sequence from differential flatness. $\mathbf{Q} = \text{blkdiag}(\mathbf{Q}_1, \mathbf{Q}_2, \mathbf{Q}_3)$ and \mathbf{R} are weight matrices. The term associated with \mathbf{Q}_1 aims to follow the reference trajectory closely. Among the diagonal elements of $\mathbf{Q}_1, \mathbf{Q}_2$, only those associated with the lateral error variable are positive to ensure the trajectory closely follows the racing line while maintaining smoothness.

Constraint (12c) imposes safety on the states by confining the lateral deviation n in a reasonable scope to avoid collisions. l_b and u_b represent the boundary of the lateral deviation n_k at the s_k^{ref} . Since the sparse Gaussian model predicts the collision interval, the left and right boundaries of the lateral error take into account the future motion of the opponent car. For example, considering the left boundary l_b :

$$l_b = \begin{cases} d_{\text{opp}}, & \text{if } c_{\text{start}} < s_k^{\text{ref}} < c_{\text{end}} \\ d_l^{\text{ref}}, & \text{otherwise} \end{cases} \quad (13)$$

where d_{opp} represents the predicted position of the opponent car and d_l^{ref} is the left boundary of the track. The future motion of the opponent vehicle is incorporated into the MPC-based QP problem (12), thereby enhancing both safety.

IV. EXPERIMENTAL RESULTS

This section evaluates the proposed FSDP method in comparison with the SOTA overtaking methods listed in Table I, focusing on overtaking success rate and trajectory feasibility.

A. Experimental Setup

The evaluation will be divided into two parts: simulation and physical verification. The simulation scene uses the default F1TENTH simulator map, and the official F1TENTH simulator [3] is used to model the behavior of a 1:10 scale racing car in real-world scenarios. The CPU used for the experiments is an AMD Ryzen 7 5800H running at 3.2 GHz. Additionally, the physical experiment was conducted on an F1TENTH racecar based on [4], using an Intel NUC as the onboard computer. The composition of the car is shown in Fig. 3. The sensor suite includes a Hokuyo UST-10LX LiDAR with a maximum scan frequency of 40 Hz. Odometry is provided by the Vedder Electronic Speed Controller (VESC). Sensor fusion combines data from the LiDAR, the IMU embedded in the VESC, and odometry, utilizing the Cartographer to localize the vehicle and obtain its state.



Fig. 3: Physical map and 1:10 scale autonomous FITENTH racing platform.

During the experiment, both the ego car and the opponent car will follow the global minimum curvature racing line [18]. The trajectory tracking controller uses a tire-dynamics-based PP controller, with tire parameters identified through an on-track system identification method [19]. To better evaluate the overtaking ability of different algorithms, we define the speed-scaler $\mathcal{S}_{\max} = \frac{v_{\text{opp}}}{v_{\text{ego}}} \in [0, 1]$. The ego vehicle consistently operates at its maximum speed v_{\max} , while the opponent vehicle runs at a speed v_{opp} lower than that of the ego vehicle. In the experiments, we evaluate different algorithms by progressively reducing the opponent's speed until the ego vehicle is able to successfully complete the overtaking maneuver. The metrics used to evaluate the algorithm's performance are as follows:

- $\mathcal{R}_{\text{ot}/c}$: The number of successful overtakes \mathcal{N}_{ot} and crashes \mathcal{N}_c were logged to compute the overtaking success rate $\mathcal{R}_{\text{ot}/c} = \frac{\mathcal{N}_{\text{ot}}}{\mathcal{N}_{\text{ot}} + \mathcal{N}_c}$.
- l : The length of overtaking trajectory.
- T : The time taken to complete the overtaking maneuver and return to the race line.
- \bar{a} : The average change rate in acceleration during overtaking.
- $\bar{\delta}$: The average rate of change of the steering angle during overtaking.

$\mathcal{R}_{\text{ot}/c}$ is used to indicate the success rate of the overtaking algorithms. l and T represent the execution efficiency of the overtaking trajectory, while \bar{a} and $\bar{\delta}$ describe the stability of the vehicle when tracking the overtaking trajectory.

B. Simulation Results

1) *Prediction*: In the simulation, a virtual opponent was generated with Gaussian noise to simulate opponent vehicles. After three laps, the proposed data selection method was compared with the *Predictive Spliner* method. The latter utilizes only the latest data for path prediction, while the proposed method integrates both new and old data, thereby better handling noise and changes in the opponent's behavior.

The dataset is limited to 400 samples to prevent it from growing indefinitely. As illustrated in Fig. 1, the position and velocity of the opponent vehicle are predicted using SGP. Taking the position prediction as an example, the training and prediction times of SGP are reduced by 60.60% and 83.93%, respectively, compared to GP, highlighting the superior real-time performance of SGP, as shown in Fig. 4.

In terms of updates to the GP dataset, as shown in Fig. 5, the proposed selection method reduces the RMSE of the

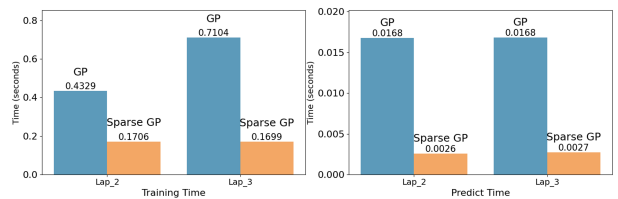


Fig. 4: Training and prediction time comparison of the original GP and the proposed SGP, evaluated on the simulation environment.

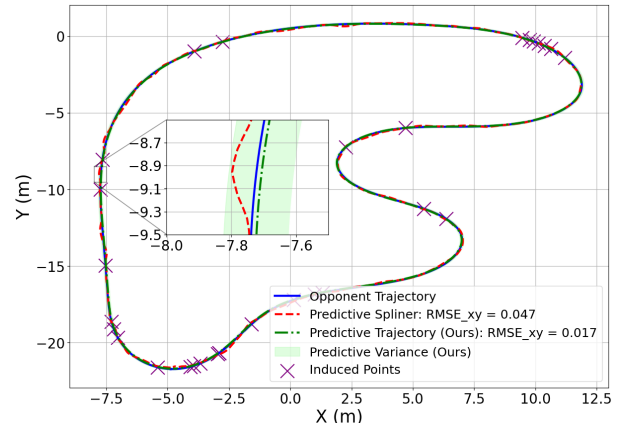


Fig. 5: Predictive trajectory comparison of the baseline *Predictive Spliner* [11] compared to the proposed FSDP prediction. The opponent's actual trajectory is depicted in blue; the baseline *Predictive Spliner* [11] in red; the proposed FSDP solution in green with the green shaded variance, as well as the induced points of the SGP in violet.

predicted trajectory by 63.83% compared to the *Predict Spliner* method, making it more closely aligned with the actual movement of the virtual opponent. The *Predict Spliner* method, relying solely on the latest data, is more vulnerable to noise interference and data distortion.

2) *Overtake*: As shown in Table II, the overtaking success rate of FSDP reached 90.90%, surpassing the performance of the listed SOTA. For the same \mathcal{S}_{\max} , the overtaking success rate of FSDP is approximately 9.09% higher than that of the *Predictive Spliner*. The average speed during overtaking is $v_o = l/T$. For FSDP, its $v_o = 4.67$ m/s the highest among SOTA methods, indicating that the trajectories it plans have higher execution efficiency. Due to the absence of dynamic opponent prediction, methods such as *Frenet*, *GBO*, and *Spliner* show lower overtaking success rates under lower values of \mathcal{S}_{\max} . Regarding trajectory quality, FSDP exhibits smaller values for \bar{a} and $\bar{\delta}$ in simulation tests. Compared to

Overtaking Planner	$\mathcal{R}_{\text{ot}/c}$ [%]	l [m]	T [s]	\bar{a} [m/s ³]	$\bar{\delta}$ [rad/s]
Frenet	57.14	13.53	3.86	237.18	0.71
GBO	57.14	15.96	5.04	443.12	0.62
Spliner	72.72	22.82	5.35	70.13	0.55
Pred. Spliner	81.81	23.15	5.23	93.64	0.50
FSDP (ours)	90.90	22.67	4.85	42.72	0.40

TABLE II: Overtaking performance of each evaluated planner in the simulation.

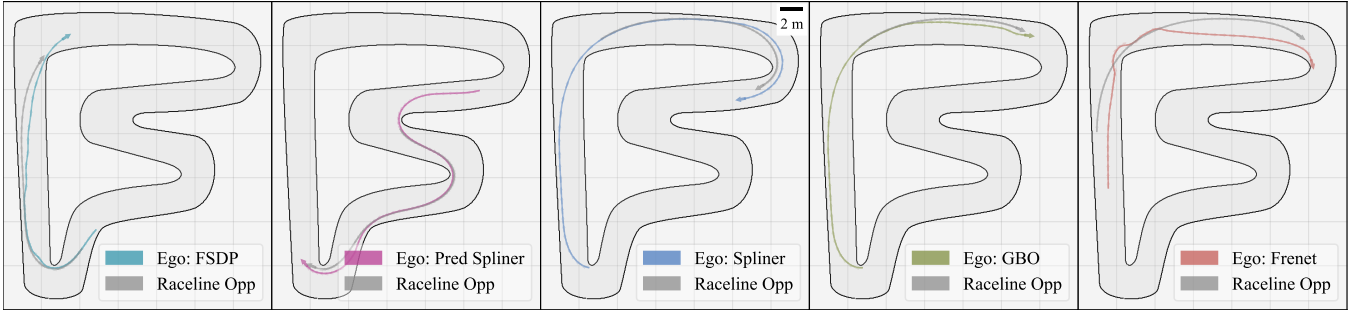


Fig. 6: Comparison of our approach with SOTA in the simulation of an overtaking maneuver. Each subplot illustrates the trajectories of the ego vehicle (colored path) and the opponent (gray path) during the maneuver. The speed scalar \mathcal{S}_{\max} for each method is as: FSDP: 53.8%, Pred. Spliner: 53.8%, Spliner: 47.5%, GBO: 30%, Frenet: 30%.

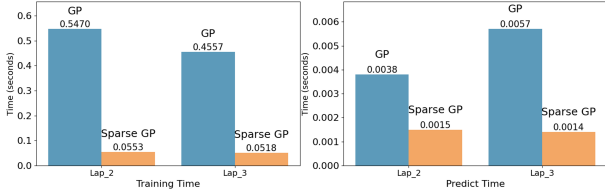


Fig. 7: Training and prediction time comparison of the original GP and the proposed SGP, evaluated on the on-board compute unit of the physical robot.

Overtaking Planner	$\mathcal{R}_{ot/c}[\%]$	$l[m]$	$T[s]$	$\bar{a}[m/s^3]$	$\bar{\delta}[rad/s]$
Frenet	62.50	5.82	3.81	1082.26	0.96
GBO	55.00	8.89	5.02	916.15	1.08
Spliner	60.00	7.18	3.02	773.54	0.81
Pred. Spliner	62.50	5.56	2.00	824.27	0.68
FSDP (ours)	71.43	5.50	2.02	218.15	0.70

TABLE III: Overtaking performance of each evaluated planner on a 1:10 scale physical autonomous racing platform.

the *Predictive Spliner*, these two metrics have decreased by 54.4% and 20.0%, respectively. This improvement can be attributed to the fact that FSDP simultaneously considers both the smoothness of the trajectory and the vehicle’s kinematic model. These results indicate that FSDP not only achieves high success rates but also ensures high performance in terms of trajectory quality. Fig. 6 visualizes the overtaking trajectories of all methods in simulation.

C. Physical Results

1) *Prediction*: In the real vehicle experiment, the same process as in the simulation was followed, where a real vehicle replaced the virtual opponent. After three laps, the data-filtering results of our method were compared with those of the *Predictive Spliner* method. With SGP, reductions in training time by 88.63%, prediction time by 60.53%, and a decrease in RMSE of the predicted trajectory by 33.87% were achieved after the data selection. The specific results are presented in Fig. 7 and Fig. 8. Results demonstrate the real-time performance of SGP, as well as the method’s ability to more accurately predict the opponent’s behavior by integrating both new and historical data.

2) *Overtake*: As shown in Table III, compared to SOTA, FSDP still demonstrates advantages in trajectory execution efficiency and smoothness. In comparison to the *Predictive*

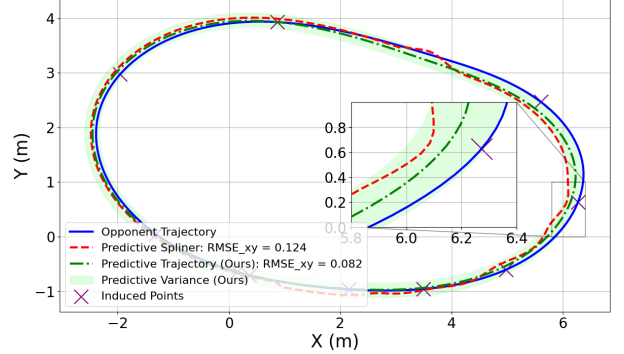


Fig. 8: Predictive trajectory comparison of the baseline *Predictive Spliner* [11] compared to the proposed FSDP prediction in the real map.

Overtaking Planner	Simulation Comp.Time [ms]		Physical Comp. Time [ms]	
	μ_c	σ_c	μ_c	σ_c
Frenet	8.88	19.16	7.03	3.30
GBO	16.03	4.58	9.20	4.87
Spliner	2.31	2.86	3.65	1.49
Pred. Spliner	40.17	33.81	45.70	39.80
FSDP (ours)	10.43	31.33	9.84	22.46

TABLE IV: Computational results of each overtaking strategy. Simulation is computed on the AMD Ryzen 7 CPU, and physical computations are done on the Intel NUC. The computational times are reported with their mean μ_c and standard deviation σ_c .

Spliner, the value of \bar{a} in FSDP decreased by 73.5%. With the highest \mathcal{S}_{\max} , FSDP achieved an overtaking success rate of 71.43% on the real vehicle, representing the best performance among the SOTA methods. Compared to the *Predictive Spliner*, the success rate of FSDP is 8.93% higher, indicating improved safety. This result indicates that the trajectory planned by FSDP offers higher safety and smoothness on real racetracks. Fig. 9 visualizes the overtaking trajectories of all methods in the real vehicle experiments, and Fig. 10 shows FSDP’s overtaking screenshot.

D. Compute

The computation time of FSDP is higher than that of *Spliner* and *Frenet*, and is roughly comparable to that of GBO. In terms of trajectory performance, FSDP far exceeds the aforementioned three methods. FSDP achieves higher

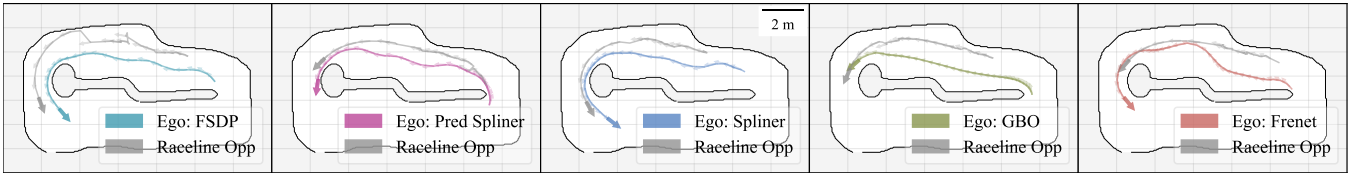


Fig. 9: Comparison of our approach with SOTA in the real experiment of an overtaking maneuver. Each subplot illustrates the trajectories of the ego vehicle (colored path) and the opponent (gray path) during the maneuver. The speed scalar \mathcal{S}_{\max} for each method is as: FSDP: 60%, Pred. Spliner: 55%, Spliner: 45%, GBO: 30%, Frenet: 30%.

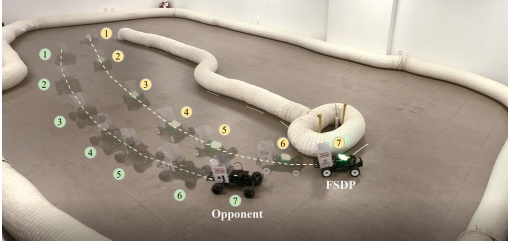


Fig. 10: FSDP's Overtaking Screenshot.

performance with a slight increase in solution time, and the results are clearly evident. Compared to the high-performing *Predictive Spliner*, FSDP's computation time was reduced by 74.04% due to its use of SGP. This demonstrates that FSDP achieves an excellent balance between performance and computation time, exhibiting outstanding performance in overtaking scenarios.

V. CONCLUSION

In this paper, we propose a data-driven overtaking algorithm for head-to-head autonomous racing competitions, named FSDP. FSDP first utilizes SGP to predict opponent behavior, and then employs a bi-level QP framework to generate the overtaking trajectory. Unlike previous approaches, FSDP ensures the vehicle's dynamics and safety while maintaining real-time performance by formulating the entire optimization problem in the Frenet frame within an MPC framework. Experiment results demonstrate that our method surpasses SOTA by achieving an 8.93% increase in overtaking success rate, supporting the maximum opponent speed among these methods, ensuring a smoother ego trajectory, and reducing 74.04% computation time compared to the *Predictive Spliner*, demonstrating its effectiveness in real-time motion planning. Future work will focus on extending our approach to scenarios involving multiple opponents, where the complexity of the planning and prediction tasks increases.

REFERENCES

- [1] A. Wischnewski, M. Geisslinger, J. Betz, T. Betz, F. Fent, A. Heilmeier, L. Hermansdorfer, T. Herrmann, S. Huch, P. Karle *et al.*, "Indy autonomous challenge-autonomous race cars at the handling limits," in *12th International Munich Chassis Symposium 2021: chassis. tech plus*. Springer, 2022, pp. 163–182.
- [2] J. Betz, H. Zheng, A. Liniger, U. Rosolia, P. Karle, M. Behl, V. Krovi, and R. Mangharam, "Autonomous vehicles on the edge: A survey on autonomous vehicle racing," *IEEE Open Journal of Intelligent Transportation Systems*, vol. 3, pp. 458–488, 2022.
- [3] M. O'Kelly, H. Zheng, A. Jain, J. Auckley, K. Luong, and R. Mangharam, "Tunercar: A superoptimization toolchain for autonomous racing," in *2020 IEEE International Conference on Robotics and Automation (ICRA)*, 2020, pp. 5356–5362.
- [4] N. Baumann, E. Ghignone, J. Kühne, N. Bastuck, J. Becker, N. Imholz, T. Kränzlin, T. Y. Lim, M. Lötscher, L. Schwarzenbach *et al.*, "Forzaeth race stack—scaled autonomous head-to-head racing on fully commercial off-the-shelf hardware," *Journal of Field Robotics*, 2024.
- [5] Z. Zhang and P. Tsotras, "Buzzracer: A palm-sized autonomous vehicle platform for testing multi-agent adversarial decision-making," in *2024 IEEE/RSJ International Conference on Intelligent Robots and Systems (IROS)*. IEEE, 2024, pp. 8510–8515.
- [6] J. Shi, T. Zhang, Z. Zong, S. Chen, J. Xin, and N. Zheng, "Task-driven autonomous driving: Balanced strategies integrating curriculum reinforcement learning and residual policy," *IEEE Robotics and Automation Letters*, 2024.
- [7] R. Trumpp, E. Javanmardi, J. Nakazato, M. Tsukada, and M. Caccamo, "Racemop: Mapless online path planning for multi-agent autonomous racing using residual policy learning," in *2024 IEEE/RSJ International Conference on Intelligent Robots and Systems (IROS)*. IEEE, 2024, pp. 8449–8456.
- [8] Y. Song, H. Lin, E. Kaufmann, P. Dürr, and D. Scaramuzza, "Autonomous overtaking in gran turismo sport using curriculum reinforcement learning," in *2021 IEEE international conference on robotics and automation (ICRA)*. IEEE, 2021, pp. 9403–9409.
- [9] E. Ghignone, N. Baumann, and M. Magno, "Tc-driver: A trajectory conditioned reinforcement learning approach to zero-shot autonomous racing," *IEEE Transactions on Field Robotics*, 2024.
- [10] Z. Demeter, M. Hell, and G. Hajgató, "Lessons learned from an autonomous race car competition," 11 2024, p. 25.
- [11] N. Baumann, E. Ghignone, C. Hu, B. Hildisch, T. Hämmerle, A. Bettoni, A. Carron, L. Xie, and M. Magno, "Predictive spliner: Data-driven overtaking in autonomous racing using opponent trajectory prediction," *IEEE Robotics and Automation Letters*, 2024.
- [12] M. Werling, J. Ziegler, S. Kammel, and S. Thrun, "Optimal trajectory generation for dynamic street scenarios in a frenet frame," in *2010 IEEE International Conference on Robotics and Automation*. IEEE, 2010, pp. 987–993.
- [13] T. Stahl, A. Wischnewski, J. Betz, and M. Lienkamp, "Multilayer graph-based trajectory planning for race vehicles in dynamic scenarios," in *2019 IEEE Intelligent Transportation Systems Conference (ITSC)*. IEEE, 2019, pp. 3149–3154.
- [14] A. Liniger, A. Domahidi, and M. Morari, "Optimization-based autonomous racing of 1:43 scale rc cars," *Optimal Control Applications and Methods*, vol. 36, no. 5, pp. 628–647, 2015.
- [15] J. Becker, N. Imholz, L. Schwarzenbach, E. Ghignone, N. Baumann, and M. Magno, "Model-and acceleration-based pursuit controller for high-performance autonomous racing," in *2023 IEEE International Conference on Robotics and Automation (ICRA)*. IEEE, 2023, pp. 5276–5283.
- [16] H. Liu, Y.-S. Ong, X. Shen, and J. Cai, "When gaussian process meets big data: A review of scalable gps," *IEEE transactions on neural networks and learning systems*, vol. 31, no. 11, pp. 4405–4423, 2020.
- [17] Z. Han, Y. Wu, T. Li, L. Zhang, L. Pei, L. Xu, C. Li, C. Ma, C. Xu, S. Shen *et al.*, "An efficient spatial-temporal trajectory planner for autonomous vehicles in unstructured environments," *IEEE Transactions on Intelligent Transportation Systems*, vol. 25, no. 2, pp. 1797–1814, 2023.
- [18] A. Heilmeier, A. Wischnewski, L. Hermansdorfer, J. Betz, M. Lienkamp, and B. Lohmann, "Minimum curvature trajectory planning and control for an autonomous race car," *Vehicle System Dynamics*, 2019.
- [19] O. Dikici, E. Ghignone, C. Hu, N. Baumann, L. Xie, A. Carron, M. Magno, and M. Corno, "Learning-based on-track system identification for scaled autonomous racing in under a minute," *IEEE Robotics and Automation Letters*, 2025.